Investigating the Microstructural and Wear Properties of Graphene-Reinforced Aluminium 6061-T6 Surface Composites Fabricated Using Friction Stir Processing

Bhargav Patel[1] D. K. Patel[2]
[1]Research Scholar [2]Professor
[1,2]Department of Mechanical Engineering
[1]Gujarat Technological University, Ahmedabad, Gujarat, India [2]Government Engineering College, Patan, Gujarat, India

Abstract — Friction Stir Processing (FSP) is a promising solid-state technique for the fabrication of surface composites with improved mechanical and tribological properties. In the present work, graphene-reinforced AA6061-T6 surface composites were fabricated using the groove filling method followed by FSP. The effects of tool rotational speed (1000 and 1200 rpm) and graphene volume fraction (15, 20, and 25 vol.%) on the microstructure and wear behavior of the composites were investigated. The distribution of graphene was found to be strongly dependent on the processing parameters. Improved material flow and more uniform reinforcement dispersion were achieved at the higher rotational speed of 1200 rpm, whereas higher graphene content resulted in localized agglomeration and defect formation in some specimens. The wear behavior showed significant dependence on both rotational speed and graphene content. Among the samples processed at 1000 rpm, the specimen containing 20 vol.% graphene exhibited lower wear compared to the other conditions. For the specimens processed at 1200 rpm, the composite reinforced with 25 vol.% graphene demonstrated the lowest wear depth and the best wear resistance. The enhanced tribological performance was attributed to the combined effects of grain refinement, improved graphene dispersion, and the formation of a protective graphene-rich tribolayer during sliding. Although variations in the coefficient of friction were observed, wear resistance was found to be more strongly influenced by microstructural integrity and reinforcement distribution.

Keywords: Friction Stir Processing, AA6061-T6, Graphene, Surface Composite, Microstructure, Wear Behaviour, Tribology

I. Introduction

Currently, aluminium, the second most abundant element in Earth's crust, is widely utilised across various industries for its advantageous mechanical properties, including lower density than steel, excellent formability, and high thermal conductivity. Surface composites retain the qualities of the base material while improved surface properties. Friction Stir Processing (FSP) is an advanced solid-state material processing technique widely employed for surface modification, microstructural refinement, and the fabrication of surface composites. Derived from friction stir welding technology, FSP utilizes a rotating tool to generate frictional heat and severe plastic deformation, resulting in localized microstructural changes without melting the base material. The process effectively refines grain structure, homogenizes the distribution of reinforcing particles, eliminates casting defects, and improves the overall mechanical and tribological properties of materials. Owing to these advantages, FSP has emerged as a promising technique for the development of high-performance surface composites and functionalized engineering materials [1–3]. Friction Stir Processing (FSP) employs a non-consumable rotating tool consisting of a shoulder and a protruding pin that actively interacts with the workpiece material. During processing, frictional heat generated by the rotating tool softens the material without reaching its melting point, while the combined action of tool rotation and traverse movement induces intense plastic deformation and material flow. This severe thermo-mechanical action leads to significant microstructural modification and grain refinement within the processed region. Consequently, distinct microstructural zones are formed, namely the Stir Zone (SZ), where the material undergoes extensive plastic deformation and dynamic recrystallization; the Thermo-Mechanically Affected Zone (TMAZ), which experiences both heat and deformation but insufficient recrystallization; and the Heat-Affected Zone (HAZ), which is influenced only by the thermal cycle without substantial plastic deformation. These regions collectively constitute the processing zone and exhibit different microstructural characteristics and mechanical properties, as illustrated in Fig. 1.

Metal Matrix Composites (MMCs) reinforced with ceramic or carbon-based particles have attracted considerable attention as potential structural materials for automotive, aerospace, marine, and defense applications. These composites exhibit superior mechanical properties, including high specific strength, elevated elastic modulus, improved wear resistance, enhanced fatigue life, and better creep resistance compared to conventional monolithic alloys. Such characteristics make MMCs suitable for components operating under demanding service conditions. However, the incorporation of hard, non-deformable reinforcement particles often leads to a reduction in ductility and fracture toughness due to stress concentration effects and limited plastic deformation of the matrix. Consequently, despite their excellent strength and stiffness, the reduced toughness and formability of MMCs remain significant challenges that restrict their widespread industrial utilization [4]. FSP offers an effective solution to these limitations by enabling controlled incorporation and uniform dispersion of reinforcements within the surface layer while simultaneously refining the matrix microstructure, thereby achieving a favourable balance between strength and ductility.

The incorporation of ceramic and carbon-based reinforcements through Friction Stir Processing (FSP) has been extensively investigated to improve the mechanical and tribological performance of aluminum alloys. The introduction of silicon carbide (SiC) particles together with graphene nanoplatelets (GNPs) and graphene oxide (GO) into an AA7075-T6 matrix using a groove-filling technique demonstrated significant enhancements in surface properties.

Under optimized processing conditions, including a tool rotational speed of 1480 rpm and a traverse speed of 30 mm/min, the hybrid composite exhibited improved microstructural refinement, higher microhardness, and superior wear resistance compared to the unreinforced alloy [5].

Similarly, the incorporation of exfoliated graphite into the A356 aluminum alloy matrix resulted in substantial improvements in hardness and wear performance. The formation of aluminum carbide (Al_4C_3) phases during processing contributed to strengthening the matrix, leading to a hardness increase of more than four times that of the base material. Furthermore, the wear rate was reduced by approximately 57%, indicating the effectiveness of carbon-based reinforcements in enhancing the tribological behavior of aluminum alloys [6].

Graphene-based reinforcements are particularly attractive due to their exceptional mechanical properties and intrinsic self-lubricating characteristics. During machining operations, graphene can reduce friction at the tool–workpiece interface, thereby lowering cutting forces and improving machinability. This lubricating effect not only enhances surface finish but also contributes to reduced tool wear and energy consumption during manufacturing processes [7].

In another study, graphene particle-reinforced AA6082-T6 surface composites fabricated through FSP exhibited significantly improved wear characteristics. Processing at a tool rotational speed of 710 rpm and a traverse speed of 63 mm/min in a single pass resulted in a more homogeneous distribution of graphene particles within the stir zone. Consequently, the processed composite showed considerably lower wear mass loss compared to both the friction stir processed alloy without reinforcement and the untreated base material, highlighting the beneficial role of graphene in improving wear resistance and surface durability [8].

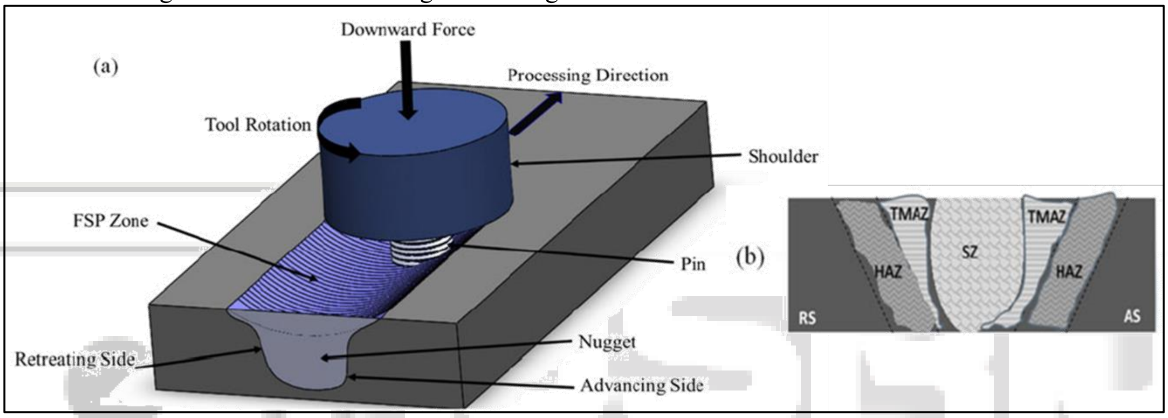

Fig. 1: (a) Principle of FSP and (b) processed zones [9]

II. METHODOLOGICAL APPROACH:

An aluminium 6061-T6 plate of 100 X 100 X 6 mm is used for the study. Graphene powder has been used as nanoparticles, whose SEM micrograph, as received from the manufacturer Add nano Technologies. The average thickness of graphene particles is 5 to 10 nm. 15, 20, and 25 volume percentage cavities were made by a square groove on the centre line of the tool rotation on the aluminium alloy 6061-T6 plate as depicted in Table 1. A screwed taper pin profile of AISI H13 tool steel with a shoulder diameter of 18 mm, with 60 concave, a pin diameter of 3 to 5 mm and a height of 4 mm was used as shown in Fig 2.

Coupon No.	Speed (rpm)	Feed (mm/min)	% Volume
A1	1000	100	15
A2	1000	100	20
A3	1000	100	25
B1	1200	100	15
B2	1200	100	20
B3	1200	100	25

Table 1: Summary of FSP process parameters

Fig. 2: Threaded taper Tool

The rotational speed of 1000 rpm and travelling speed of 100 mm/min are used for the capping pass to close the groove to avoid the escapement of graphene particles during the stirring process. The experiments were carried out on a BMV-50-TC24 3 Axis Fixed Column Vertical Machining Centre. To hold the Al 6061-T6 plate, a fixture is designed and fabricated. The schematic diagram of the fixture is shown in Fig 3.

Fig. 3: CNC milling machine with fixture

The cross-section of the FSP specimens was subjected to macro- and microstructural investigations. The microstructure examination was carried out on an Olympus Digital microscope (DSX 1000). Tribological properties were studied using a pin-on disc wear rotary tribotester (DUCOM Material Characterization Instruments) under technically dry friction conditions. A 6 mm-diameter pin was cut at the centerline of the stir zone (SZ). The pin was secured in the hemispherical fixture to ensure proper contact with the steel disc at a constant rate. The velocity is 1 m/s for 1000 m.

III. Findings and Discussion:

A. Microstructure Evolution

The optical micrographs of the friction stir processed (FSP) specimens containing different graphene volume fractions at tool rotational speeds of 1000 rpm (A-series) and 1200 rpm (B-series) are presented in Fig 4. The microstructural features reveal the material flow behavior, particle distribution, and consolidation quality within the stir zone (SZ). The morphology of the graphene-rich regions is strongly influenced by the reinforcement content and processing parameters.

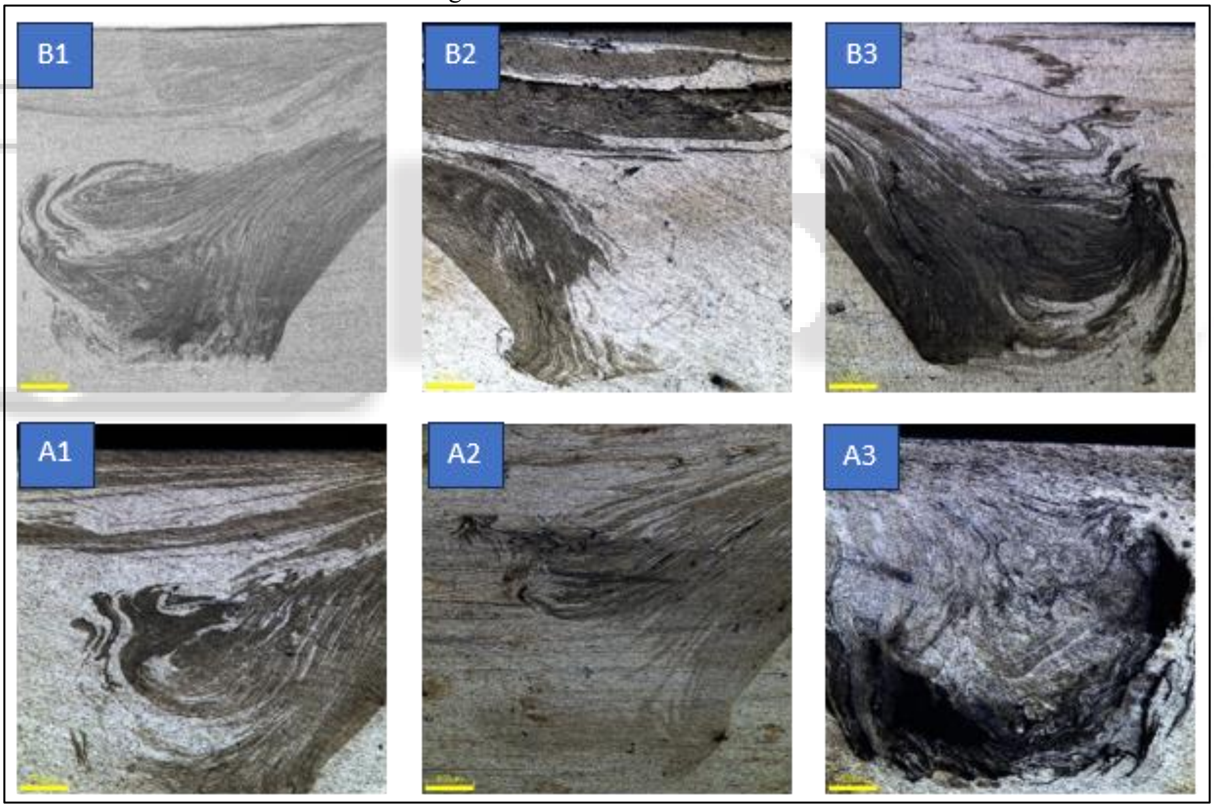

Fig. 4: Optical microscopy of the Fsped samples

For the specimens processed at 1000 rpm (A1–A3), the graphene particles are distributed in a characteristic onion-ring or vortex-like pattern within the stir zone. In sample A1 (15 vol.% graphene), a relatively compact and continuous graphene-rich region is observed, indicating effective material flow and adequate particle entrainment. The reinforcement appears reasonably well distributed, with limited clustering. This suggests that the selected processing parameters provided sufficient heat generation and plastic deformation for particle incorporation.

When the graphene content was increased to 20 vol.% (A2), the stir zone exhibited a more elongated particle flow pattern. Although graphene dispersion was still achieved, the reinforcement-rich bands became more pronounced, indicating the onset of particle agglomeration. The increased particle concentration hindered the plastic flow of the matrix material, resulting in localized non-uniformity within the processed region.

For A3 (25 vol.% graphene), significant particle accumulation and cavity formation are evident. Large dark regions and discontinuities can be observed within the stir zone, suggesting inadequate consolidation and poor bonding between the matrix and reinforcement. The excessive graphene content likely restricted material flow and reduced the effectiveness of stirring action, leading to tunnel-like defects and reinforcement clustering. These defects may adversely affect the mechanical properties of the composite.

The specimens processed at the higher rotational speed of 1200 rpm (B1–B3) exhibit comparatively improved material mixing due to increased heat generation and enhanced plasticization of the matrix. In B1 (15 vol.% graphene), a well-defined vortex structure is observed, indicating effective stirring and uniform distribution of graphene within the aluminum matrix. The reinforcement-rich region appears more refined than that of A1, suggesting improved dispersion resulting from the higher rotational speed.

For B2 (20 vol.% graphene), the microstructure shows a relatively homogeneous distribution of reinforcement with fewer visible agglomerates compared to A2. The increased rotational speed promoted stronger material flow and particle fragmentation, resulting in better incorporation of graphene into the matrix. Consequently, B2 exhibits one of the most uniform microstructures among all specimens.

In B3 (25 vol.% graphene), although the material flow pattern remains visible, considerable graphene accumulation is observed in the lower portion of the stir zone. The excessive reinforcement content exceeds the carrying capacity of the plasticized material, leading to localized clustering and non-uniform distribution. However, the defects appear less severe than those observed in A3, indicating that the higher rotational speed partially compensated for the adverse effects of increased graphene content.

Overall, the microstructural observations indicate that both rotational speed and graphene volume fraction significantly influence reinforcement distribution and stir zone integrity. Increasing the rotational speed from 1000 rpm to 1200 rpm improved material flow, enhanced particle dispersion, and reduced defect formation. Conversely, increasing the graphene content from 15 vol.% to 25 vol.% increased the tendency for particle agglomeration and cavity formation. Among the investigated conditions, B2 (1200 rpm, 20 vol.% graphene) exhibited the most homogeneous reinforcement distribution and defect-free microstructure, suggesting an optimum balance between heat input, material flow, and reinforcement content. This improved microstructural uniformity is expected to contribute positively to the mechanical and tribological performance of the developed surface composite.

B. Wear Properties

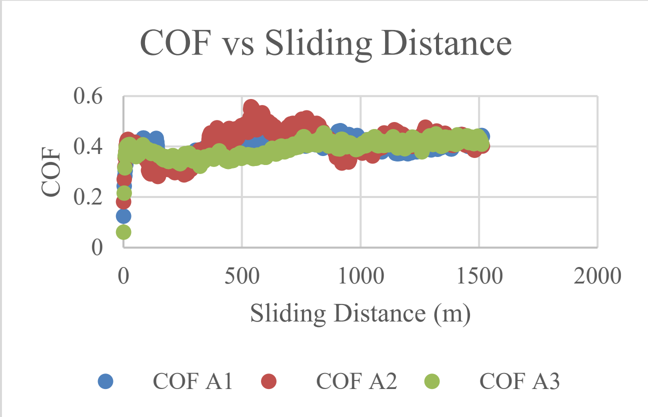

Fig. 5: COF of (A1-A3) samples

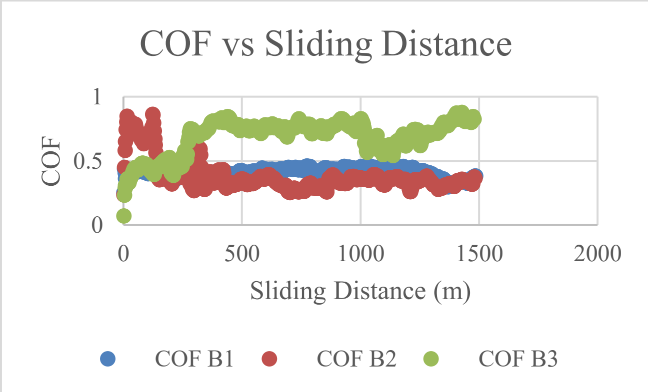

Fig. 6: COF of (B1-B3) samples

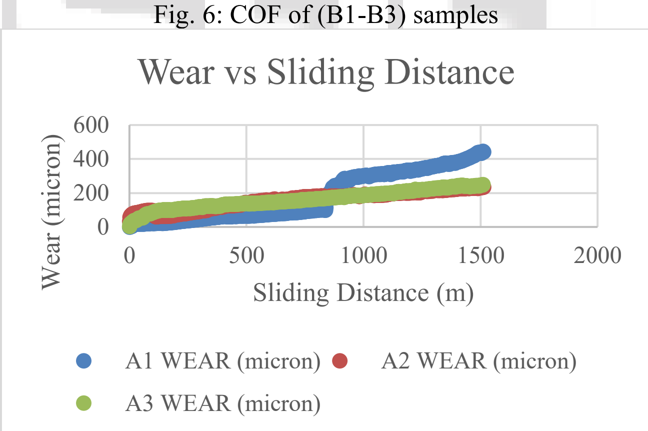

Fig. 7: Wear loss of (A1-A3)

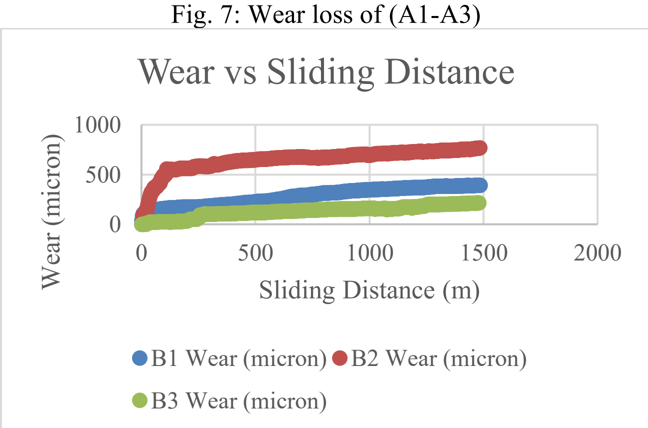

Fig. 8: Wear loss of (B1-B3)

The wear behavior of the friction stir processed AA6061-T6/graphene surface composites was evaluated by monitoring the wear depth and coefficient of friction (COF) as a function of sliding distance. The results reveal that both graphene volume fraction and tool rotational speed significantly influence the tribological performance of the processed composites.

Figure 7 shows the variation of wear with sliding distance for samples A1, A2, and A3 processed at a rotational speed of 1000 rpm. All specimens exhibited a progressive increase in wear with increasing sliding distance; however, the wear rate varied considerably among the samples. Sample A1 (15 vol.% graphene) displayed the highest cumulative wear, reaching approximately 445 µm at the end of the test. A sharp increase in wear after approximately 850 m of sliding distance indicates the onset of severe wear, likely caused by the breakdown of the protective tribolayer and direct metal-to-metal contact. Sample A2 (20 vol.% graphene) exhibited substantially lower wear, with a final wear depth of approximately 230 µm. The improved wear resistance can be attributed to the lubricating effect of graphene and its more effective distribution within the aluminum matrix, which reduced surface damage during sliding. Sample A3 (25 vol.% graphene) showed intermediate wear behavior with a final wear depth of approximately 250 µm. Although the higher graphene content provided lubrication, excessive reinforcement likely promoted agglomeration and microstructural defects, as observed in the optical micrographs, thereby limiting the wear improvement. The COF curves for the A-series specimens indicate relatively stable friction behavior after the running-in stage. The average COF remained within the range of 0.35–0.50, suggesting the formation of a stable transfer layer during sliding. Among the samples, A2 exhibited slightly higher fluctuations in COF, whereas A3 maintained comparatively smoother friction behavior due to the increased presence of lubricating graphene particles.

The wear behaviour of specimens processed at 1200 rpm is shown in Figure 8. A clear influence of rotational speed on wear performance is evident. Sample B1 (15 vol.% graphene) exhibited a final wear depth of approximately 390 µm, which is lower than that of A1. The reduction in wear can be attributed to improved particle dispersion and enhanced microstructural refinement resulting from the higher heat input and more intense material flow at 1200 rpm. In contrast, B2 (20 vol.% graphene) showed the highest wear among all specimens, reaching approximately 770 µm. The rapid increase in wear depth during the initial stages of sliding suggests instability of the surface layer and accelerated material removal. This behavior may be associated with localized particle pull-out and abrasive wear resulting from reinforcement clustering. The best wear resistance was observed for B3 (25 vol.% graphene), which exhibited the lowest wear depth of approximately 210 µm after 1500 m of sliding. The superior performance is attributed to the combined effects of enhanced graphene content and improved particle dispersion at the higher rotational speed, leading to the formation of a stable lubricating tribofilm that effectively reduced material loss.

The wear performance of the composites is governed by the synergistic effects of graphene reinforcement, microstructural refinement induced by FSP, and the quality of particle distribution within the stir zone. Graphene acts as a solid lubricant, reducing direct asperity contact and promoting the formation of a protective tribolayer. However, excessive reinforcement content can result in particle agglomeration and processing defects, which may serve as crack initiation sites and accelerate wear. The microstructural observations showed that samples processed at higher rotational speed exhibited improved material flow and reinforcement distribution. Consequently, the specimen B3 (1200 rpm, 25 vol.% graphene) achieved the most favorable balance between lubrication, load-bearing capability, and microstructural homogeneity, resulting in the highest wear resistance among all tested conditions. Overall, the wear results demonstrate that the tribological behavior of FSPed AA6061-T6/graphene composites is strongly dependent on both processing parameters and reinforcement content. The optimum wear performance was achieved for the specimen processed at 1200 rpm with 25 vol.% graphene (B3), whereas the poorest wear resistance was observed for B2, indicating that uniform reinforcement distribution is more critical than reinforcement content alone in determining wear behavior.

IV. CONCLUSION

The present study investigated the fabrication of graphene-reinforced AA6061-T6 surface composites through Friction Stir Processing (FSP) at tool rotational speeds of 1000 rpm and 1200 rpm with graphene volume fractions of 15%, 20%, and 25%. Based on the microstructural and tribological analyses, the following conclusions can be drawn:

- FSP successfully incorporated graphene into the AA6061-T6 matrix and produced a distinct stir zone characterized by vortex-like material flow patterns. The distribution of graphene was strongly influenced by both rotational speed and reinforcement content.
- Increasing the rotational speed from 1000 rpm to 1200 rpm improved material plasticization and particle dispersion, resulting in a more homogeneous microstructure and reduced reinforcement clustering.
- At higher graphene contents (25 vol.%), particle agglomeration and localized defects were observed, particularly in specimens processed at lower rotational speed, indicating that excessive reinforcement can adversely affect material flow and consolidation.
- Wear resistance of the composites was significantly influenced by the combined effect of processing parameters and graphene content. Among the specimens processed at 1000 rpm, A2 and A3 exhibited lower wear than A1, demonstrating the beneficial role of graphene in reducing material loss during sliding.
- The specimen processed at 1200 rpm with 25 vol.% graphene (B3) exhibited the lowest wear depth among all tested samples, indicating superior tribological performance. The improved wear resistance is attributed to enhanced graphene dispersion, grain refinement, and

the formation of a protective graphene-rich tribolayer during sliding.

- Coefficient of friction values varied with processing conditions and reinforcement content; however, a lower coefficient of friction did not always correspond to lower wear. This suggests that microstructural integrity, reinforcement distribution, and tribofilm stability play a more dominant role in controlling wear behavior.

REFERENCES:

[1] V. Sharma, U. Prakash, and B. V. M. Kumar, "Surface composites by friction stir processing: A review," J Mater Process Technol, vol. 224, pp. 117–134, Oct. 2015, doi: 10.1016/j.jmatprotec.2015.04.019.
[2] Z. Y. Ma, "Friction Stir Processing Technology: A Review," Metallurgical and Materials Transactions A, vol. 39, no. 3, pp. 642–658, Mar. 2008, doi: 10.1007/s11661-007-9459-0.
[3] R. A. Kumar, R. G. A. Kumar, K. A. Ahamed, B. D. Alstyn, and V. Vignesh, "Review of Friction Stir Processing of Aluminium Alloys," Mater Today Proc, vol. 16, pp. 1048–1054, 2019, doi: 10.1016/j.matpr.2019.05.194.
[4] Z. Y. M. I. C. R.S. Mishra *, "Friction stir processing: a novel technique for fabrication of surface composite," Materials Science and Engineering, pp. 307–310, 2003.
[5] Vickram K, Somasundaram K. Enhancing surface properties of AA7075-T6 using carbonaceous and ceramic nanoparticle reinforcement. Welding International. 2025;1–26.
[6] Shekari A, Daneshifar MH, Allahbakhsh A. Superior tribological properties of highly-loaded graphite/A356 surface composites fabricated using friction stir processing. Tribol Int. 2024;199:110049.
[7] Prabhakar GVNB, Dumpala L, Ravi Kumar N. Investigating Mechanical Properties, Corrosion Resistance and Machining Characteristics of Al5083-Graphene Composites Produced by Friction Stir Processing. Transactions of the Indian Institute of Metals. 2020;73(12):2955–2964.
[8] Peddavarapu S, Muthu Veerappan A, Raghuraman S. Tribological study of Graphene reinforced AA6082 surface composite processed through Friction Stir Processing. Mater Today Proc. 2020;27:2225–2229.
[9] V. Patel, W. Li, A. Vairis, and V. Badheka, "Recent Development in Friction Stir Processing as a Solid-State Grain Refinement Technique: Microstructural Evolution and Property Enhancement," Critical Reviews in Solid State and Materials Sciences, vol. 44, no. 5, pp. 378–426, Sep. 2019, doi: 10.1080/10408436.2018.1490251.